Inorganic Chemistry

Article

pubs.acs.org/IC

Triple-Stranded Helicates of Zinc(II) and Cadmium(II) Involving a New Redox-Active Multiring Nitrogenous Heterocyclic Ligand: Synthesis, Structure, and Electrochemical and Photophysical Properties

Nabanita Kundu,[†] Sk Md Towsif Abtab,[†] Sanchita Kundu,[†] Akira Endo,[‡] Simon J. Teat,[§] and Muktimoy Chaudhury*,[†]

[†]Department of Inorganic Chemistry, Indian Association for the Cultivation of Science, Kolkata 700 032, India

[‡]Department of Materials and Life Sciences, Faculty of Science and Technology, Sophia University, 7-1 Kioi-cho, Chioda-ku, Tokyo 102-8554, Japan

[§]Advanced Light Source, Lawrence Berkeley National Laboratory, 1 Cyclotron Road, Mail Stop 2-400, Berkeley, California 94720, United States

Supporting Information

ABSTRACT: The protonated form $[H_2(L)](CF_3SO_3)_2$ (**1**) of a new redox-active bis-bidentate nitrogenous heterocyclic ligand, viz., 3,3′-dipyridin-2-yl[1,1′]bi[imidazo[1,5-*a*]pyridinyl] (L), and its zinc(II) and cadmium(II) complexes (**2** and **3**) have been synthesized and characterized by single-crystal X-ray diffraction analysis. In the solid state, both **2** and **3** have triple-stranded helical structures involving ligands that experience twisting and bending to the extent needed by the stereoelectronic demand of the central metal ion. The metal centers in the zinc(II) complex $[Zn_2(L)_3](ClO_4)_4$ (**2**) are equivalent, each having a distorted octahedral geometry, flattened along the C_3 axis with a Zn1···Zn1# separation of 4.8655(13) Å. The cadmium complex $[Cd_2(L)_3(H_2O)](ClO_4)_4$ (**3**), on the other hand, has a rare type of helical structure, showing coordination asymmetry around the metal centers with a drastically reduced Cd1···Cd2 separation of 4.070 Å. The coordination environment around Cd1 is a distorted pentagonal bipyramid involving a N_6O donor set with the oxygen atom coming from a coordinated water, leaving the remaining metal center Cd2 with a distorted octahedral geometry. The structures of **2** and **3** also involve anion−π- and CH−π-type noncovalent interactions that play dominant roles in shaping the extended structures of these molecules in the solid state. In solution, these compounds exhibit strong fluxional behavior, making the individual ligand strands indistinguishable from one another, as revealed from their ^{1}H NMR spectra, which also provide indications about these molecules retaining their helical structures in solution. Electrochemically, these compounds are quite interesting, undergoing ligand-based oxidations in two successive one-electron steps at $E_{1/2}$ of ca. 0.65 and 0.90 V versus a Ag/AgCl (3 M NaCl) reference. These molecules are all efficient emitters in the red and blue regions because of ligand-based $\pi^*-\pi$ fluorescent emissions, tuned appropriately by the attached Lewis acid centers.

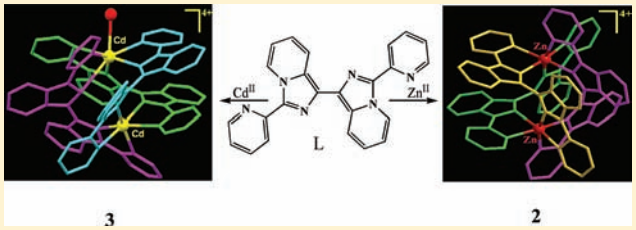

INTRODUCTION

The metal-assisted self-assembly of helicates is a topic of burgeoning interest in contemporary coordination chemistry research[1−4] because of their biomimetic relevance and aesthetic appeal.[1a−c,3] Studies on the basic mechanism and the energetics of their formation, structure, and properties of helicates help one to understand the fundamental principles of molecular recognition and self-organization,[2] which are important for the rational design of more complex architectures.[1,3a,5] Among the various classes of ligands that are shown to be suitable for the construction of different types of helicates,[6] polypyridines are particularly numerous.[1b,c,7−10] Many transition-metal assemblies with such ligands display intense photoluminescence. This property renders these compounds to become promising candidates in the fields of biological imaging, photochemical catalysis, molecular optical and electronic devices, chemical sensors, and light-driven fuel production.[11−15] In this context, d^{10} luminophores deserve special mention owing to their better performance in sensor technology and electroluminescent devices[15,16] because these compounds are strongly emissive under UV radiation and the emission energies can span over a broad spectral range.[17]

Coordination complexes of π-electron-deficient heteroaromatic ligands are often accompanied by unique noncovalent interactions like anion−π,[18] $\pi-\pi$,[19] and lone pair−π[20] interactions. Such noncovalent interactions play a significant role in both chemical and biological recognition.[21] We have recently synthesized[22] a π-electron-deficient N-heterocyclic compound, viz., 3,3′-dipyridin-2-yl[1,1′]bi[imidazo[1,5-*a*] pyridinyl] (L) containing a pair of biologically relevant[23] imidazo[1,5-*a*]pyridine moieties. The ligand L is redox-active

Received: December 2, 2011
Published: January 26, 2012

 © 2012 American Chemical Society dx.doi.org/10.1021/ic202595p | *Inorg. Chem.* 2012, 51, 2652−2661

Table 1. Summary of X-ray Crystallographic Data for Complexes 1−3

parameter	1	2·2.25H_2O	3·0.5H_2O
composition	$C_{26}H_{18}N_6O_6F_6S_2$	$C_{72}H_{52.5}Cl_4N_{18}O_{18.25}Zn_2$	$C_{72}H_{51}N_{18}O_{17.5}Cl_4Cd_2$
fw	688.58	1734.36	1814.91
cryst syst	monoclinic	monoclinic	triclinic
space group	$P2_1/c$	$C2/c$	$P\bar{1}$
a, Å	5.3667(8)	23.725(4)	10.9650(15)
b, Å	17.057(3)	13.5241(19)	15.101(2)
c, Å	15.106(2)	23.990(4)	22.596(3)
α, deg	90.0	90.0	91.733(2)
β, deg	98.553(6)	109.466(3)	96.585(3)
γ, deg	90.0	90.0	106.162(2)
V, Å^3	1367.4(4)	7257(2)	3562.3(8)
D_{calc}, Mg m^{-3}	1.672	1.587	1.692
temp, K	296(2)	193(2)	193(2)
λ, Å	0.710 73	0.774 90	0.774 90
Z	2	4	2
$F(000)$, μ mm^{-1}	700/0.292	3538/1.126	1826/1.038
$2\theta_{max}$, deg	67.38	51.52	51.26
reflns collected/unique	15 115/5056	14 947/5360	26 166/10350
R_{int}	0.0847	0.0486	0.0629
no. of param	208	565	1108
R1(F_o), wR2(F_o) [$I \geq 2\sigma(I)$]	0.0909, 0.2087	0.0524, 0.1350	0.0729, 0.1859
R1(F_o^2), wR2(F_o^2) (all data)	0.2158, 0.2752	0.0714, 0.1471	0.1017, 0.2011
GOF on F^2	1.314	1.018	1.072

and capable of acting as a bis-bidentate ligand, and its copper(II) compound offers a unique example of valence tautomerism in solution.[24] Herein, we report the synthesis of the protonated form of this ligand as well as its zinc(II) and cadmium(II) complexes. The compounds have been characterized by single-crystal X-ray diffraction analysis as well as by NMR and electrospray ionization mass spectroscopy (ESI-MS). In addition, the redox behavior and emission properties of these complexes have been investigated.

EXPERIMENTAL SECTION

Materials. The ligand L was prepared as described elsewhere.[22] All other reagents were commercially available and used as received. Solvents were reagent-grade and were dried from the appropriate reagents[25] and distilled under nitrogen prior to their use.

Preparation of Compounds. *[H_2(L)](CF_3SO_3)$_2$ (1).* An acetonitrile solution (5 mL) of trifluoromethanesulfonic acid was carefully layered onto a solution of the ligand L in dichloromethane (5 mL), forming two distinct layers. Diffusion between these two layers over a period of 3 weeks produced a dark-red crystalline compound. Yield: 85%. Anal. Calcd for $C_{26}H_{18}F_6N_6O_6S_2$: C, 45.35; H, 2.63; N, 12.20. Found: C, 45.02; H, 2.57; N, 12.11. FT-IR bands (KBr pellets, cm^{-1}): 3506, 3149, 2921, 1620, 1585, 1542, 1487, 1398, 1271, 1249, 1176, 1149, 1031, 756, 640. UV−vis [CH_3CN; λ_{max}, nm (ε, L mol^{-1} cm^{-1})]: 496 (25 300), 305 (19 300), 290 (19 800).

[Zn_2(L)$_3$](ClO_4)$_4$·2.25H_2O (2·2.25H_2O). A methanolic solution (5 mL) of Zn(ClO_4)$_2$·6H_2O (40 mg, 0.1 mmol) was carefully poured onto a solution of the ligand L (40 mg, 0.1 mmol) in dichloromethane (5 mL), forming two distinct layers. Diffusion between these two layers over a period of 5 days produced a yellow crystalline compound. Some of these crystals were of diffraction grade and were kept with the mother liquor to prevent loss of any interstitial solvent. Drying under vacuum for a long time afforded a fully desolvated sample, used for various measurements including microanalysis. Yield: 41 mg (48%). Anal. Calcd for $C_{72}H_{48}Cl_4N_{18}O_{16}Zn_2$: C, 51.05; H, 2.86; N, 14.88. Found: C, 50.65; H, 2.91; N, 14.72. FT-IR bands (KBr pellets, cm^{-1}): 3504, 1600, 1487, 1461, 1315, 1251, 1089, 783, 748, 700, 624. ESI-MS (positive) in CH_3CN: m/z 1204.65 [Zn_2(L)$_2$(ClO_4)$_3$]$^+$, 941.05 [Zn(L)$_2$$ClO_4$]$^+$, 420.07 [Zn(L)$_2$]$^{2+}$, 226.01 [Zn(L)]$^{2+}$.

[Cd_2(L)$_3$(H_2O)](ClO_4)$_4$·0.5H_2O (3·0.5H_2O). To a stirred acetone solution (10 mL) of the ligand L (235 mg, 0.6 mmol) was added Cd(ClO_4)$_2$·6H_2O (170 mg, 0.4 mmol) taken in acetone (10 mL). The mixture was stirred for a period of 2 days to get a deep-yellow solution. It was then filtered. The filtrate was layered with petroleum ether (60−80 °C fraction) and was allowed to stand at 4 °C in a refrigerator for about 3 days. The yellow crystalline compound deposited at this stage was collected by filtration. Some of these crystals were of diffraction grade and were kept with the mother liquor to prevent the loss of interstitial solvent. Drying under vacuum at room temperature over $CaCl_2$ afforded a fully desolvated sample, used for various measurements including microanalysis. Yield: 150 mg (43%). Anal. Calcd for $C_{72}H_{50}N_{18}Cl_4O_{17}Cd_2$: C, 47.94; H, 2.77; N, 13.98. Found: C, 47.69; H, 2.80; N, 13.77. FT-IR bands (KBr pellets, cm^{-1}): 3589, 2923, 1639, 1596, 1485, 1460, 1373, 1313, 1249, 1087, 781, 748, 669, 621. UV−vis [CH_3CN; λ_{max}, nm (ε, L mol^{-1} cm^{-1})]: 371 (29 500), 269 (43 200).

Caution! *Perchlorate salts of metal complexes containing organic ligands are potentially explosive[26] and should be handled in small quantities with sufficient care.*

Physical Measurements. Elemental (C, H, and N) analyses were performed at IACS on a Perkin-Elmer model 2400 series II CHNS analyzer. ^{1}H NMR spectra were recorded using Bruker model Avance DPX 300 and Bruker Avance 600 spectrometers at ambient temperature. ^{113}Cd NMR spectra were obtained on a JEOL Lambda 500 NMR spectrometer with the data analysis system (ALICE) operating at ambient temperature (299 K). Cadmium acetate was used as the external reference (δ_0). Emission spectra in solution as well as in the solid state were recorded on a Perkin-Elmer LS55 luminescence spectrophotometer. UV−vis, IR, and ESI-MS spectra were recorded using the same instrumentation facilities as those described elsewhere.[27] Cyclic voltammetry in *N*,*N*-dimethylformamide (DMF) was recorded on a BAS model 100 B/W electrochemical workstation using a platinum disk (i.d. = 1.6 mm) working electrode and a platinum wire counter electrode. Ag/AgCl (3 M NaCl) was used for the reference and a Fc/Fc$^+$ couple as the internal standard.[28] Solutions were ∼1.0 mM in samples and contained 0.1 M tetrabutylammonium perchlorate (TBAP) as the supporting electrolyte. Bulk electrolyses were carried out using a platinum-gauze working electrode at 298 K.

X-ray Crystallography. Diffraction-quality crystals of **1** (needle-like, red, 0.28 mm × 0.02 mm × 0.01 mm), **2** (platelike, yellow, 0.12

dx.doi.org/10.1021/ic202595p | Inorg. Chem. 2012, 51, 2652−2661

mm × 0.08 mm × 0.01 mm), and **3** (needlelike, yellow, 0.3 mm × 0.02 mm × 0.01 mm) were collected from their respective reaction pot. Crystals were mounted on glass fibers and aligned on a Bruker Platinum 200 CCD diffractometer in the case of **2** and **3**, while a SMART APEX II CCD diffractometer was employed for **1**. Solvent-losing crystals (**2** and **3**) were coated with paraffin oil and were placed in the cold stream of liquid nitrogen for low-temperature data collection. Intensity data were collected with silicon 111 monochromatized synchrotron radiation (λ = 0.774 90 Å) at 193(2) K using the ω-rotation scan techniques with narrow frames for **2** and **3**. Intensity data for compound **1** were measured by employing a monochromatized Mo Kα radiation (λ = 0.710 73 Å) source using ϕ and ω scan techniques at 296(2) K. No crystal decay was observed during the data collections. Intensity data were corrected for empirical absorption. In all cases, absorption corrections based on multiscans using *SADABS* software[29] were applied. The structures were solved by direct methods,[30] and least-squares refinements [anisotropic displacement parameters, hydrogen atoms (except those bound to water) in the riding model approximation, and a weighing scheme of the form $w = 1/[\sigma^2(F_o^2) + (aP)^2 + bP]$ for $P = (F_o^2 + 2F_c^2)/3$] were on F^2.[30] Bruker *SHELXTL*[31] was used for both structure solutions and refinements. A summary of the relevant crystallographic data and the final refinement details are given in Table 1. All non-hydrogen atoms were refined anisotropically. Geometrical and displacement parameter restraints were used in modeling the perchlorate counterions (for **2** and **3**). Hydrogen atoms were placed geometrically and constrained using a riding model, except for the water-bound hydrogen atoms. These hydrogen atoms could neither be placed nor found in the difference map and were omitted from the refinements. The *SMART* and *SAINT* software packages[32] were used for data collection and reduction, respectively. Crystallographic diagrams were drawn using the *DIAMOND* software package.[33]

RESULTS AND DISCUSSION

Syntheses. The protocol followed for the synthesis of **1**−**3** is summarized in Scheme 1. The ligand L has identical halves,

Scheme 1. Protocol Followed for the Synthesis of Compounds 1−3

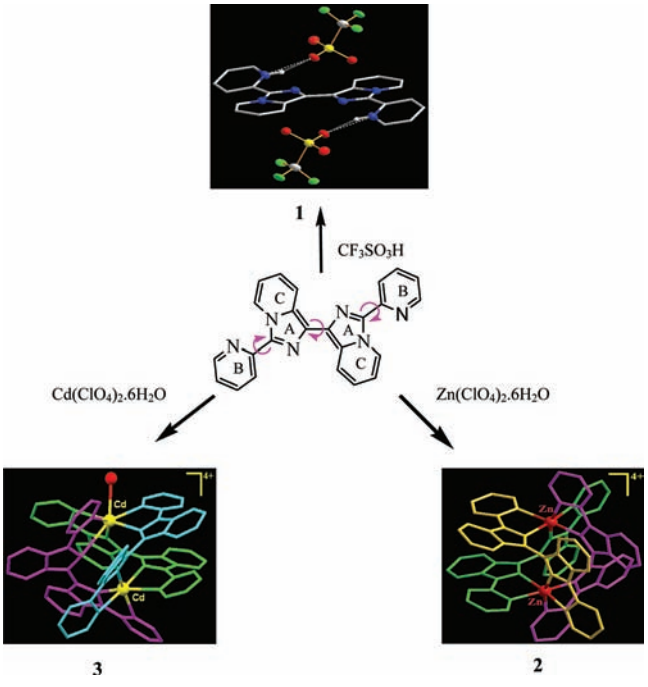

each containing three different heterocyclic rings, viz., imidazole (A), isolated pyridine (B), and fused pyridine (C) rings, which will be designated as im, py, and azopy rings, respectively, in the following part of this discussion. Like other linear oligopyridine molecules, the present N-heterocyclic ligand (L) is also a grossly planar molecule in the solid state with a transoid arrangement of the donor nitrogen atoms about their respective interannular C−C bonds (shown in Figure 1a,b).[22] During its coordination to a metal ion, the donor nitrogen atoms adopt cisoid conformations (Figure 1c,d) about the interannular C−C bonds.[34] In addition, the stereoelectronic demands of the individual metal ions can also control the extent of twist and bending around the C−C bond between central aromatic rings of L to generate complexes with different helical topologies. Both zinc(II) and cadmium(II) ions form dinuclear triple-stranded helicates in **2** and **3**. Of particular interest here is the larger size of the cadmium(II) ion, which needs an additional water molecule to complete a seven-coordination geometry around one of the metal sites in **3**, thus generating a rare variety of triple-stranded helicate with a homotopic ligand, showing coordination asymmetry at the metal centers. Interestingly, the ligand L in combination with H^+, which may be regarded as a metal ion (Lewis acid) of very small size with no specific stereochemical preference, generates an almost planar molecule $[H_2(L)](CF_3SO_3)_2$ (**1**). Orientation of the rings in this compound as revealed from its crystal structure (see later) indicates a grossly planar structure with cisoid conformations for the terminal imidazopyridine moieties.

IR spectra of complexes **1**−**3** contain all of the pertinent bands of the N-heterocyclic ligand L appearing at ca. 1600, 1485, 1461, 1313, 1247, and 770 cm^{-1}. Compound **1** displays a strong band at 1240 cm^{-1} due to a $CF_3SO_3^-$ counteranion.[35] A couple of strong bands appearing at ca. 1089 and 624 cm^{-1} in **2** and **3** provide the signature for the ClO_4^- counteranion.[35]

The ESI-MS spectrum (positive ion mode) recorded in acetonitrile for compound **2** is displayed in Figure 2. The highest mass cluster corresponding to the cation $[Zn_2(L)_2(ClO_4)_3]^+$ is obtained at m/z 1204.65 with this compound. It also displays peaks due to other ionic species, viz., $[Zn(L)_2ClO_4]^+$, $[Zn(L)_2]^{2+}$, and $[Zn(L)]^{2+}$ at m/z 941.05, 420.07, and 226.01, respectively. The observed isotopic distributions and their simulation patterns are in agreement with these assigned formulations, as shown in Figure 2 for a representative signal. Compounds **1** and **3**, however, appeared to be fragile under the conditions of ESI-MS ionization and failed to provide the corresponding molecular-ion peaks.

Description of Crystal Structures. The molecular structure and atom labeling scheme for compound **1** is shown in Figure 3, and the relevant metrical parameters are compiled in Table S1 (in the Supporting Information). The compound crystallizes in the monoclinic space group $P2_1/c$ with two molecular weight units accommodated per cell. It has a 2-fold axis of symmetry. The cationic part exhibits a cis−trans−cis conformation about the sequential interannular C−C bonds. The central im rings lie in a unique plane (dihedral angle 0°), while the terminal py rings, unlike in the free ligand,[22] deviate from the central plane (dihedral angle 15.35°) of the molecule. The cis conformation of the adjacent py and im rings (with donor nitrogen atoms N1 and N4, both facing the proton H5A) is driven by their attachment to the incoming proton H5A. The observed cisoid conformations of the py−im domains are stabilized by the short contact distances of the hydrogen-bonded triflate anion (O2---H5A, 2.129 Å) with pyridine nitrogen atom N1 (O2---N1, 2.856 Å) and im nitrogen atom N4 (O2---N4, 3.646 Å; Figure 3). Protonation also has a

dx.doi.org/10.1021/ic202595p | Inorg. Chem. 2012, 51, 2652−2661

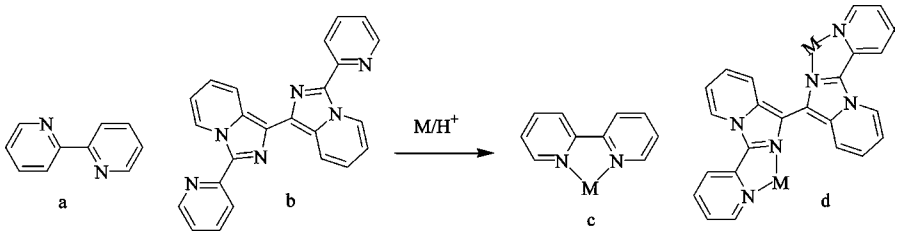

Figure 1. Schematic representations of the transoid conformations of the free ligands (a) 2,2′-bipyridine and (b) L, while parts c and d represent the corresponding cisoid conformations of these two molecules in the presence of metal ions or H^+.

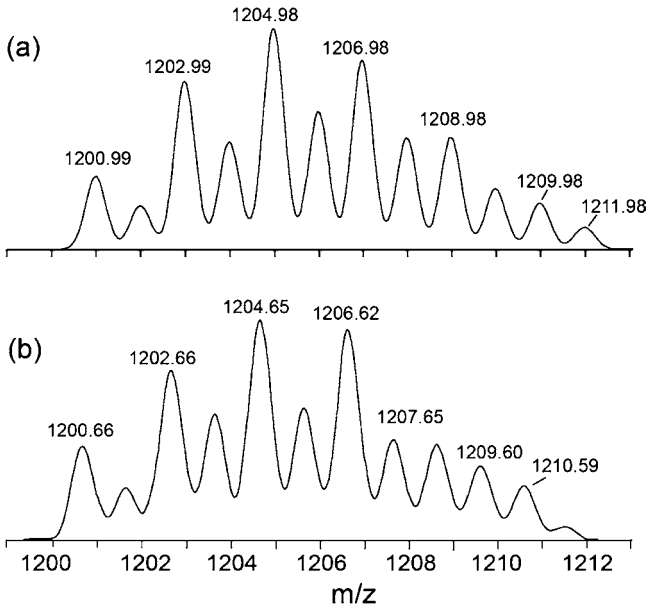

Figure 2. Peak corresponding to the cation $[Zn_2(L)_2(ClO_4)_3]^+$ in the ESI-MS spectrum (positive) for complex **2** in acetonitrile with simulated (above, a) and observed (below, b) isotopic distributions.

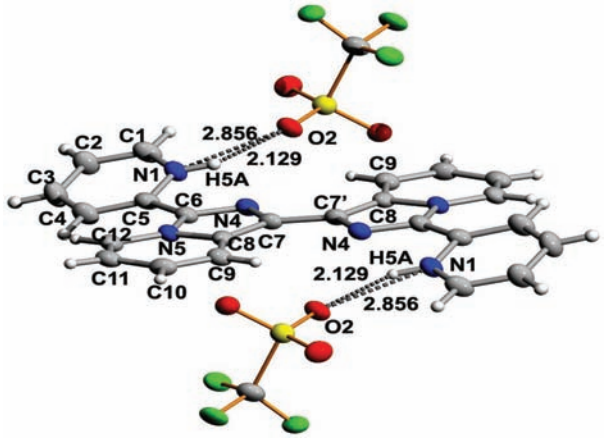

Figure 3. Molecular structure with an atom labeling scheme for the protonated form **1** of the ligand.

stake in the nonplanar structure of this molecule, as reflected from the lowering of the bridge angles between the py and im rings (N1−C5−C6, 114.10°; N4−C6−C5, 120.81°), which are smaller than the angle between the central im−im rings (C8−C7−C7′, 127.56°; N4−C7′−C7, 122.28°].

The perspective view of the molecular structure of **2** with an atomic labeling scheme as well as the one using a space-filling model are shown in Figures 4 and S1 (in the Supporting

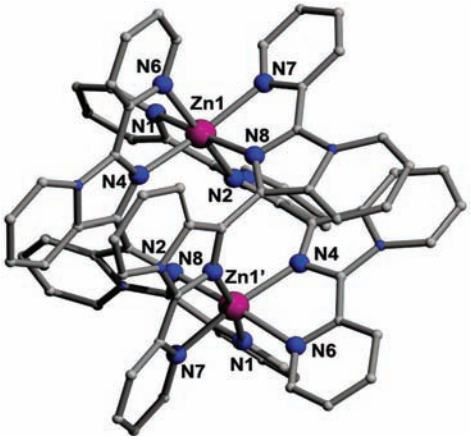

Figure 4. Wire-frame presentation with an atomic labeling scheme of the triple-helical structure of the cation in **2**. Each ligand is shown in a different color.

Information), respectively, which provide confirmatory evidence in support of its dinuclear triple-helical structure. Some selected metrical parameters are displayed in Table 2. The

Table 2. Selected Bond Distances (Å) and Angles (deg) for 2[a]

Bond Distances (Å)			
Zn1−N1A	2.180(5)	Zn1−N2A	2.193(4)
Zn1−N4	2.120(4)	Zn1−N6	2.210(5)
Zn1−N7	2.187(5)	Zn1−N8	2.131(5)
Bond Angles (deg)			
N1A−Zn1−N2A	77.24(17)	N1A−Zn1−N4	90.77(17)
N1A−Zn1−N6	96.26(18)	N1A−Zn1−N7	98.30(19)
N1A−Zn1−N8	170.91(18)	N2A−Zn1−N4	104.53(17)
N2A−Zn1−N6	173.37(17)	N2A−Zn1−N7	89.04(17)
N2A−Zn1−N8	95.01(17)	N4−Zn1−N6	76.56(17)
N4−Zn1−N7	165.12(17)	N4−Zn1−N8	95.82(17)
N6−Zn1−N7	90.68(18)	N6−Zn1−N8	91.36(17)
N7−Zn1−N8	76.60(18)		

[a]Symmetry operation of equivalent atoms: A, $-x$, y, $-z + {}^1/_2$.

compound crystallizes in the monoclinic space group $C2/c$ with four molecular weight units accommodated per cell. The presence of a crystallographic inversion center implies the equivalence of the zinc(II) centers in this molecule. The cation has an approximate D_3 symmetry with three bis-bidentate ligands getting wrapped around the Zn−Zn axis in such a way as to give the zinc(II) cation a distorted octahedral geometry, which is defined by three py and three im nitrogen atoms, so that the donor set is in a *cis*-N_6 conformation. Four donor atoms (N1, N4, N7, and N8) from the ligand strands occupy

dx.doi.org/10.1021/ic202595p | *Inorg. Chem.* 2012, 51, 2652−2661

the basal plane and lie −0.163, 0.171, 0.188, and −0.196 Å, respectively, out of the least-squares plane through them. The apical positions are taken up by the N2 and N6 donor atoms. The trans angles N1−Zn−N8 [170.91(18)°], N2−Zn−N6 [173.37(17)°], and N4−Zn−N7 [165.12(17)°] are close to linearity. As a result of small N(im)−Zn−N(py) bite angles [76.56(17)−77.24(17)°] within each chelate, the coordination spheres around the zinc(II) center may be described as octahedra flattened along the C_3 axis, where each zinc(II) atom is displaced by 0.050 Å out of their least-squares basal plane toward the center of the molecule. The Zn−N bond distances [2.120(4)−2.210(5) Å] are in the expected range.[36] The three ligand strands in **2** are twisted to different extents (by 85.74°, 67.11°, and 67.11°) about their central C−C (im−im) bond to generate helicity in the molecule. The Zn1···Zn1# separation is 4.866 Å. In addition, an all-cisoid nitrogen-donor conformation of the molecule brings two im rings and two azopy rings into closer proximity [interplanar distances 3.372(4) and 3.649(4) Å, respectively]. Such small interplanar distances generate extensive intramolecular $\pi-\pi$-stacking interactions between the adjacent ligand strands along with anion−π interactions involving the perchlorate anion (Figure S2 in the Supporting Information). These $\pi-\pi$-stacking interactions are of the classical type,[37] as judged by the dihedral angles of 3.45° and 0° between the im−im and azopy−azopy π planes, respectively.

Crystal and molecular structures of **3** along with its space-filling model are shown in parts a and b of Figure 5,

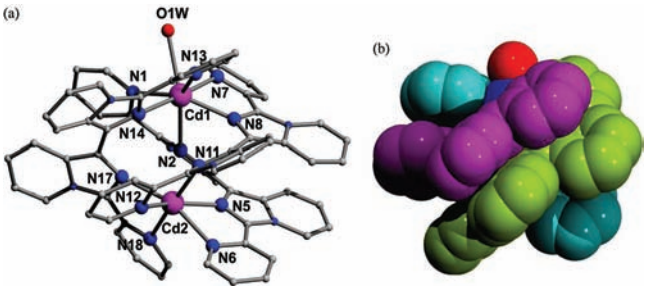

Figure 5. (a) Wire-frame with an atomic labeling scheme and (b) a space-filling representation of the triple-helical structure of the cation in **3**, showing coordination assymmetry. Each ligand is shown in a different color.

respectively. Relevant metrical parameters are summarized in Table 3. The compound crystallizes in the triclinic space group $P\bar{1}$ with two molecular weight units accommodated per cell. The dinuclear cation $[Cd_2(L)_3(H_2O)]^{4+}$ adopts a triple-helical structure, where the three ligand strands are twisted to different extents (42.44°, 38.34°, and 33.33°) about their central interannular C−C (im−im) bond and are wrapped around a pseudo-C_3 axis passing through the metal ions. The coordination environment around Cd1 is best described as a distorted pentagonal bipyramid with a N_6O donor unit in which the basal plane is occupied by four nitrogen atoms (N1, N8, N13, and N2) coming from the bis-bidentate ligands and an oxygen atom (O1W) contributed by a coordinated water molecule. The epical positions are taken up by N7 and N14 atoms. The cis angles in the basal plane are in the range 67.5(3)−80.0(3)°, showing moderate deviations from the ideal angle of 72° that force the Cd1 atom out of the least-squares basal plane by 0.179 Å toward the center of the molecule. The trans angle N7−Cd1−N14, 171.9(3)°, is close to linearity. The coordination environment around Cd2, on the other hand, is

Table 3. Selected Bond Distances (Å) and Angles (deg) for 3

Bond Distances (Å)			
Cd1−O1W	2.476(8)	Cd2−N5	2.266(8)
Cd1−N7	2.458(8)	Cd2−N11	2.332(7)
Cd1−N13	2.447(8)	Cd2−N17	2.332(7)
Cd1−N1	2.363(8)	Cd2−N6	2.447(8)
Cd1−N8	2.287(8)	Cd2−N12	2.381(8)
Cd1−N14	2.377(7)	Cd2−N18	2.383(8)
Cd1−N2	2.763(9)		
Bond Angles (deg)			
O1W−Cd1−N1	79.7(3)	N5−Cd2−N6	69.8(3)
O1W−Cd1−N8	124.1(3)	N5−Cd2−N12	152.9(3)
O1W−Cd1−N14	97.3(3)	N5−Cd2−N18	83.7(3)
N1−Cd1−N8	142.6(3)	N6−Cd2−N12	86.7(3)
N1−Cd1−N14	83.4(3)	N6−Cd2−N18	99.3(3)
N7−Cd1−N13	117.5(3)	N11−Cd2−N17	110.1(3)
N8−Cd1−N13	80.0(3)	N12−Cd2−N17	82.1(3)
N13−Cd1−N14	69.7(3)	N17−Cd2−N18	71.7(3)
O1W−Cd1−N7	82.0(3)	N5−Cd2−N11	90.9(2)
O1W−Cd1−N13	72.0(3)	N5−Cd2−N17	124.2(3)
N1−Cd1−N7	88.5(3)	N6−Cd2−N11	80.6(3)
N1−Cd1−N13	137.4(3)	N6−Cd2−N17	160.8(3)
N7−Cd1−N8	69.5(3)	N11−Cd2−N12	71.5(2)
N7−Cd1−N14	171.9(3)	N11−Cd2−N18	174.3(2)
N8−Cd1−N14	116.9(3)	N12−Cd2−N18	114.2(3)

distorted octahedral, with four basal positions being taken up by N11, N18, N5, and N12 atoms. The epical sites are occupied by N6 and N17 atoms, contributed also by the ligand strands. One of the trans angles in the basal plane N12−Cd2−N5, 152.9(3)°, is considerably short of linearity, and the Cd2 atom is shifted by 0.192 Å out of the least-squares basal plane toward the center of the molecule. These displacements of Cd1 and Cd2 toward the center reduces the separation between the metal centers (Cd1---Cd2 distance 4.070 Å) to an appreciable extent. The Cd−N bond distances [2.266(8)−2.458(8) Å] except Cd1−N2 are in the expected range,[38] and the bond lengths to the im nitrogen atoms are shorter than the bond lengths to pyridine nitrogen donor atoms. The Cd1−O1W bond length, 2.476(8) Å, is only slightly larger than that normally found in other cadmium(II) compounds.[39] The Cd1−N2 bond length, 2.763(9) Å, is longer than normal Cd−N bonds but much shorter than the sum of the corresponding van der Waals radii (4.04 Å), indicating that the Cd1 center is seven-coordinated.

The remarkable features in the structure of **3** are the presence of hither to unknown anion−$\pi-\pi-\pi-\pi$−anion and −anion−$\pi-\pi-\pi-\pi$−anion−$\pi-\pi-\pi-\pi$−anion−$\pi-\pi-\pi-\pi$− chain interactions. As depicted in Figure 6a, O32 and the disordered O33 (O33′) oxygen atoms of perchlorate ions interact simultaneously with one face of an intramolecularly stacked $\pi_{azopy}-\pi_{azopy}$ aromatic ring system, which, in turn, is involved in intermolecular $\pi-\pi$-stacking interactions with the azopy ring of another tetracation, thus generating an anion $\pi-\pi-\pi-\pi$−anion interaction (Figure 6b). The O33 (O33′) and O32---ring plane distances are in the range 3.04(2)−3.665(17) Å, reflecting strong-to-moderate anion−π interactions.[18n] The intramolecular $\pi_{centroid}-\pi_{centroid}$ and intermolecular $\pi_{centroid}-\pi_{centroid}$ distances are 3.543(6) and 3.875(7) Å, respectively. The perchlorate oxygen atom O33 again has established O33−$\pi-\pi-\pi-\pi$−O33 interactions (Figure 6b) involving a similar type of intra- and intermolecular face-to-face

dx.doi.org/10.1021/ic202595p | Inorg. Chem. 2012, 51, 2652−2661

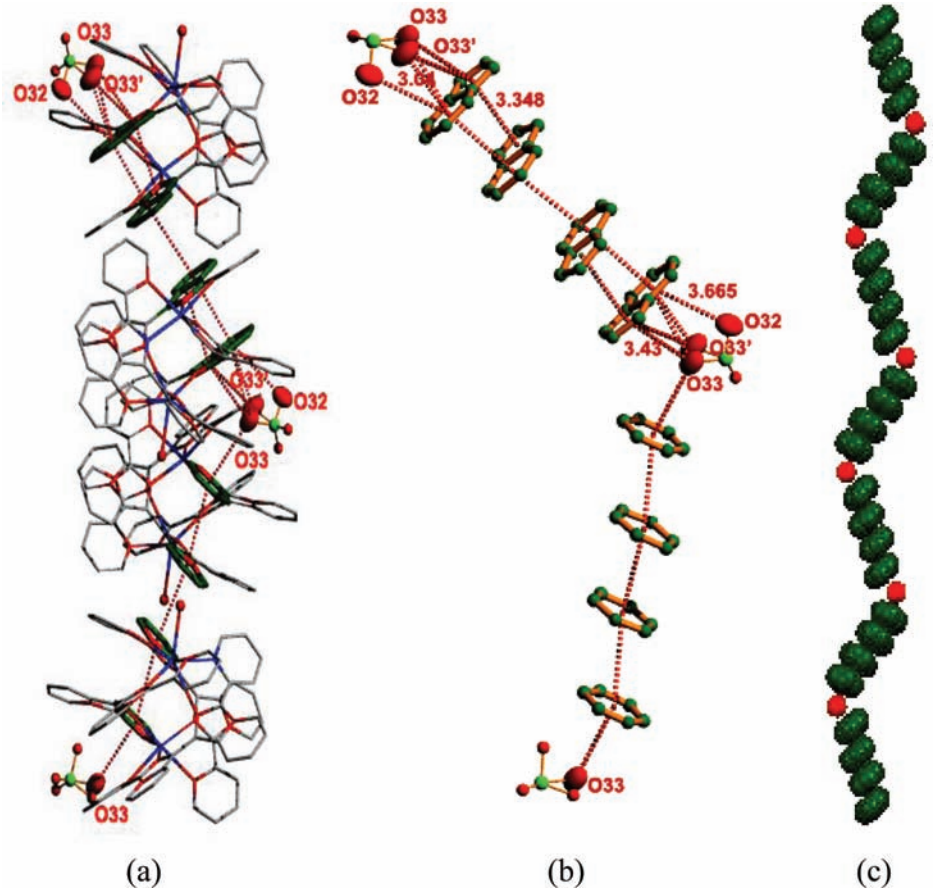

Figure 6. (a) Crystallographic evidence for the rare multiple −anion−π−π−π−π−anion−π−π−π−π−anion−π−π−π−π− chain interactions in **3**. Three perspective views are shown in parts a−c. In part b, the nonrelevant atoms have been omitted for clarity, and in part c, a view of the 1D helical chain generated by these chain interactions is displayed.

Table 4. ^{1}H NMR Spectral Data (δ, ppm)[a] at Room Temperature for the Free Ligand L and Complexes 2 and 3

L[b]		2[b]		3[b]		Assignments
10.04 (7.3) d	2H	7.99 (4.8) d	2H	8.02 (3.8) d	2H	H1, H1′
8.81 (9.0) d	2H	7.73 (8.2) d	2H	7.58 (8.0) d	2H	H4, H4′
8.68 (4.7) d	2H	8.36 (7.2) d	2H	8.40 (6.6) d	2H	H5, H5′
8.53 (8.1) d	2H	6.38 (9.1) d	2H	6.84 (8.1) d	2H	H8, H8′
7.88 (7.7, 1.60) dt	2H	7.02 (8.9) t	2H	7.12 m[c]	2H	H7, H7′
7.24 (5.4) t	2H	7.11 (6.6) t	2H	7.12 m[c]	2H	H6, H6′
7.03 (8.8) t	2H	8.06 (7.8) t	2H	7.79 (7.9) t	2H	H3, H3′
6.84 (6.3) t	2H	7.34 (7.4) t	2H	7.12 m[c]	2H	H2, H2′

[a]Chemical shifts (δ) relative to internal tetramethylsilane. Proton labels are as shown in the insets in Figure 7: d, doublet; t, triplet; dt, doublet of triplet; m, multiplet. Values in parentheses represent the coupling constants (J in Hz). [b]Spectrum recorded in acetonitrile-d_3. [c]H7, H7′, H6, H6′, H2, and H2′ protons exists together as multiplets in **3**.

(F-type) π stacking. Intramolecular π−π stacking exists between a py ring and an azopy ring, while the intermolecular stacking involves two azopy rings. The intra- and intermolecular $\pi_{centroid}$−$\pi_{centroid}$ distances are 3.862(6) and 3.623(6) Å, respectively (Table S2 in the Supporting Information). Simultaneous interactions of O33 with two π−π−π−π-stacked moieties generate an −anion−π−π−π−π−anion−π−π−π−π−anion−π−π−π−π− oligomeric arrangement with a helical topology (Figure 6c).

^{1}H NMR Spectroscopy. The ^{1}H NMR spectra of **2** and **3** in acetonitrile-d_3 have been recorded at room temperature, and the data are summarized in Table 4. For comparison, the data for the free ligand (L) are also included in that table. The spectrum of **2** (Figure 7) contains four doublets and four triplets in the region of 8.37−6.36 ppm. Assignments of these signals become straightforward when compared with the corresponding 2D ^{1}H−^{1}H correlation spectrum (Figure S3 in the Supporting Information). The pyridine protons H2 and H3 (proton labels are as shown in Figure 7, inset) are shifted downfield ($\Delta\delta$ = 0.5 and 1.03 ppm, respectively, with respect to the free ligand), as expected for a typical N coordination from a pyridine ring.[40] The remaining pyridine ring protons H1 and H4 and the two fused pyridine ring (azopy) protons H7 and H8 are significantly shielded in **2** ($\Delta\delta$ = 2.05, 1.08, 0.86, and 2.15 ppm, respectively). This is as expected from its triple-helical structure (vide supra) in which the pyridine ring protons

dx.doi.org/10.1021/ic202595p | Inorg. Chem. 2012, 51, 2652−2661

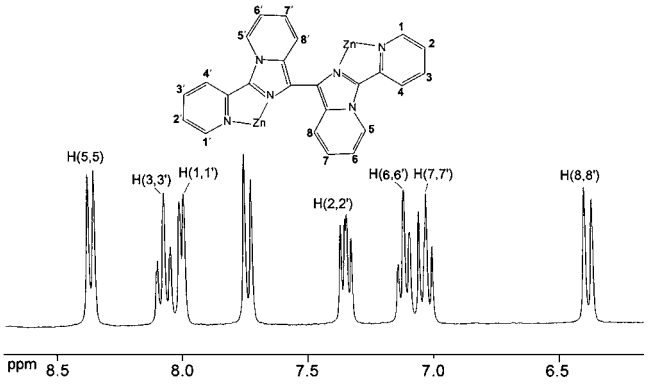

Figure 7. 300 MHz ^{1}H NMR spectrum of **2** in acetonitrile-d_3 at 293 K.

H1 and H4 and the azopyridine ring protons of one ligand strand are held within the shielding regions of the aromatic rings of the other ligand strands. The rest of the protons H5 and H6 belonging to the azopyridine ring are only marginally modified and are shielded in the complex to give signals at 8.36 and 7.11 ppm ($\Delta\delta$ = 0.32 and 0.13 ppm, respectively). Thus, the triple-helical structure that leads to intramolecular π-stacking interactions as observed in the solid state appears to be retained in solution also.

Almost a similar ^{1}H NMR spectrum (Figure S4 in the Supporting Information) is obtained for the cadmium(II) complex, except for minor chemical shift differences (Table 4) due to a more flattened structure of **3**, which enforces the aromatic rings in this compound to come closer relative to its zinc(II) counterpart. The corresponding 2D correlation spectrum (Figure S5 in the Supporting Information) is used as a guide for a complete interpretation of this spectrum.

Finally, as revealed from Figures 7 and S4 in the Supporting Information, the ^{1}H NMR spectra of **2** and **3** in solution at room temperature are perfectly symmetric. The molecular structures of these compounds in the solid state show that the different ligand strands are twisted to different extents about their central C−C (im−im) bond and some rings are more closely stacked than the others. The symmetric nature of the spectra indicates that the structures are showing fluxional behavior on the NMR time scale, giving an average structure in solution in which all of the three ligands appear to undergo the same degree of twist and π-stacking interactions.

^{113}Cd NMR Spectroscopy. To understand more about the solution structure of **3**, the ^{113}Cd NMR spectrum of the complex has been recorded in CD_3CN at room temperature. The spectrum as displayed in Figure S6 in the Supporting Information features a strong singlet at 197.93 ppm. The result clearly indicates that both cadmium(II) centers in **3** have an identical coordination environment when present in solution, unlike in the solid state.

Electrochemistry. The electrochemical behaviors of complexes **2** and **3** have been examined by cyclic voltammetry (CV) in DMF (0.1 M TBAP) using a platinum working electrode under an envelope of purified dinitrogen at 25 °C in the potential range of −2.0 to +2.0 V versus a Ag/AgCl (3 M NaCl) reference. The voltammetric features are roughly identical for both of these compounds. The cyclic and normal-pulse voltammograms of **2** in the potential range 0 to +1.2 V are displayed in Figure 8 as representative examples. The corresponding figure for **3** is displayed in Figure S7 in the Supporting Information. The voltammogram includes two

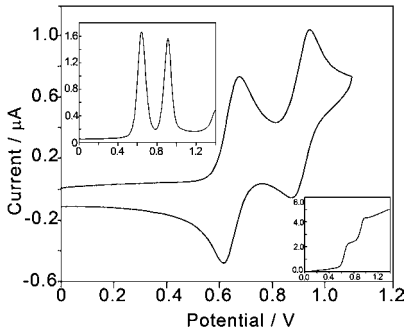

Figure 8. Cyclic voltammogram of **2** in a DMF solution (0.1 M TBAP) at 298 K; potentials versus Ag/AgCl (3 M NaCl), at a platinum working electrode; scan rate 100 mV s^{-1}. The insets show the differential- and normal-pulse voltammograms, establishing the involvement of an identical number of electron(s) for both processes I and II.

electrochemical responses at $(E_{1/2})_I$ = 0.64 V (process I) and $(E_{1/2})_{II}$ = 0.91 V (process II) involving identical number of electrons. Corresponding potentials are 0.66 and 0.90 V for **3**. On the basis of a comparison with a ferrocenium/ferrocene couple (ΔE_p, 70 mV at 100 mV s^{-1})[28] as well as using the criteria of the scan rate (50−500 mV s^{-1}) dependence of the peak current and width and equivalence of the cathodic and anodic peak current heights, processes I and II (ΔE_p, 62 and 75 mV for **2** and 60 and 56 mV for **3** at 100 mV s^{-1} for processes I and II, respectively) may be appropriately described as reversible,[41] involving a single electron. Both processes are anodic, as judged by the steady-state voltammetry (using an ultramicro platinum electrode, 10 μM in diameter). The cyclic voltammogram for the free ligand L reveals two reversible oxidation couples appearing at 56 and 78 mV versus a Ag/AgCl reference in DMF.[22] Taking a cue from that study, processes I and II for complexes **2** and **3** may be regarded as arising from the ligand-based electron transfers presented by eqs 1 and 2

$$[M^{II}{}_2(L)_3]^{4+} \underset{(E_{1/2})_I = 0.65V}{\overset{-e^-}{\rightleftharpoons}} [M^{II}{}_2(L^{\bullet})^{+}(L)_2]^{5+} \quad (1)$$

$$[M^{II}{}_2(L^{\bullet})^{+}(L)_2]^{5+} \underset{(E_{1/2})_{II} = 0.90V}{\overset{-e^-}{\rightleftharpoons}} [M^{II}{}_2(L^{\bullet\bullet})^{2+}(L)_2]^{6+} \quad (2)$$

where M = Zn or Cd.

The electron stoichiometries for these couples in compound **2** were confirmed by constant-potential coulometric experiments with a platinum gauze working electrode. Exhaustive electrolysis past the first oxidation process (E_w = +0.75 V) established a single-electron stoichiometry (n = 0.95 ± 0.06 F mol^{-1}) for this couple. Similar experiments for the second oxidation process (E_w = +1.10 V), however, did not yield any meaningful results because of unidentified electrode reaction(s). Nevertheless, the monoelectronic nature of the latter process has been established from the normal- and differential-pulse voltammetry experiments that display identical current heights for both couples, as shown in Figure 8 (insets). The electrochemical results are thus consistent with two successive ligand-based one-electron oxidation steps, as depicted by eqs 1 and 2.

dx.doi.org/10.1021/ic202595p | Inorg. Chem. 2012, 51, 2652−2661

Luminescent Properties. The luminescent properties of compounds **1**−**3** have been investigated in solution (CH_2Cl_2/CH_3CN, 1:100, v/v) as well as in the solid state. The spectra in solution are displayed in Figure S8 in the Supporting Information, and those in the solid state, together with that of the free ligand L, are shown in Figure 9. Despite the similarities (between **2** and **3**) of their spectra in solution, the emission spectra of the compounds in the solid state are quite different. The emission maximum of L is red-shifted by 30 nm compared to that in solution. Compounds **2** and **3** display a blue shift in the fluorescence energy in going from the solution to the solid state with λ_{max} at 456 and 471 nm, respectively, thus providing the appearance of blue luminescence. Compound **1**, on the other hand, exhibits a bright-red emission band with a maximum at 618 nm, showing a red shift of 58 nm from its emission in solution. The lifetimes of these solid-state emissions are close to 2.9 ns for the main component, suggesting that luminescence of the compounds is probably caused by $\pi^*-\pi$ transitions. The excitation band maxima of the compounds are in the range 396−429 nm. Therefore, the compounds in the solid state exhibit intriguing fluorescence character, transforming UV and violet light to blue or red fluorescence. The deviations of the solid-state emissions from those in solutions are likely to originate from the crystal packing differences of the compounds in the solid state. Diverse noncovalent supramolecular interactions, viz., large numbers of $\pi-\pi$-stacking, anion$-\pi$, and lone pair$-\pi$ interactions, are likely to have causative influences in the shift of the emission energy, observed in the solid state.

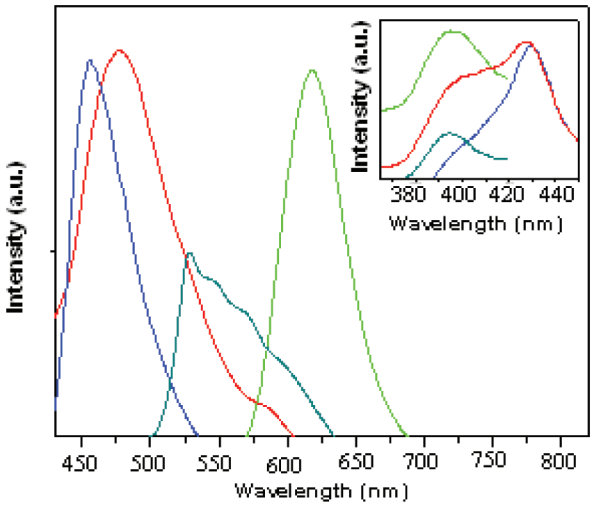

Figure 9. Emission spectra of L and **1**−**3** in the solid state at room temperature: L (dark-green line), **1** (light-green line), **2** (blue line), and **3** (red line). Inset: excitation spectra of the compounds.

CONCLUSIONS

The protonated form (**1**) of the ligand L and its coordination complexes with zinc(II) and cadmium(II) (**2** and **3**) have been synthesized. The complexes are binuclear with triple-stranded helical topology and significantly altered distances between the metal centers (4.865 Å in **2** vs 4.070 Å in **3**); all of these are controlled by the stereoelectronic demand of the central metal ions. The helicity in **3** is quite unique, showing coordination asymmetry around the cadmium(II) centers. The structures in the solid state also involve multiple anion$-\pi$ interactions, extending up to several aromatic π systems. These noncovalent interactions play dominant roles in shaping the extended structures of these compounds in the solid state. In solution, however, both **2** and **3** exhibit fluxional behavior making the individual ligand strands indistinguishable from one another as revealed from ^{1}H NMR spectroscopy. Electrochemically, these compounds (**2** and **3**) are also interesting, undergoing ligand-based oxidations in two successive single-electron steps. The compounds (**1**−**3**) are all efficient emitters in the blue and red regions, respectively, because of ligand-based $\pi^*-\pi$ fluorescent emissions, tuned appropriately by the attached Lewis acid centers, be it metal or hydrogen ions.

ASSOCIATED CONTENT

Supporting Information

Metrical parameters of **1** (Table S1), weak-interaction parameters of **1**−**3** (Table S2), space-filling presentation and weak interactions in the structure of **2** (Figures S1 and S2), ^{1}H−^{1}H COSY NMR spectra of **2** and **3** and ^{1}H and ^{113}Cd NMR spectra of **3** (Figures S3−S6), cyclic voltammogram for **3** (Figure S7), emission spectra in a solution of **1**−**3** (Figure S8), and X-ray crystallographic files in CIF format for compounds **1**−**3**. This material is available free of charge via the Internet at http://pubs.acs.org.

AUTHOR INFORMATION

Corresponding Author

*E-mail: icmc@iacs.res.in.

ACKNOWLEDGMENTS

This work was supported by the Council of Scientific and Industrial Research (CSIR), New Delhi, India. N.K., S.M.T.A., and S.K. also thank the CSIR for the award of research fellowships. The single-crystal X-ray diffraction data were recorded (in part) on an instrument supported by DST, New Delhi, India, as a National Facility at IACS under the IRHPA program. The Advanced Light Source is supported by the Director, Office of Science, Office of Basic Energy Sciences, of the U.S. Department of Energy under Contract DE-AC02-05CH11231.

REFERENCES

(1) (a) Hannon, M. J.; Childs, L. J. *Supramol. Chem.* **2004**, *16*, 7. (b) Albrecht, M. *Chem. Rev.* **2001**, *101*, 3457. (c) Piguet, C.; Bernardinelli, G.; Hopfgartner, G. *Chem. Rev.* **1997**, *97*, 2005. (d) Yeh, R. M.; Davis, A. V.; Raymond, K. N. In *Comprehensive Coordination Chemistry II*; McCleverty, J. A., Meyer, T. J., Eds.; Elsevier Ltd.: Oxford, U.K., 2004; Vol. 7, p 327. (e) von Zelewsky, A. *Stereochemistry of Coordination Compounds*; John Wiley & Sons: New York, 1996; pp 177−201.

(2) (a) Piguet, C.; Borkovec, M.; Hamacek, J.; Zeckert, K. *Coord. Chem. Rev.* **2005**, *249*, 705. (b) Hamacek, J.; Borkovec, M.; Piguet, C. *Chem.—Eur. J.* **2005**, *11*, 5217. (c) Hamacek, J.; Borkovec, M.; Piguet, C. *Chem.—Eur. J.* **2005**, *11*, 5227.

(3) (a) Lehn, J.-M. *Supramolecular Chemistry: Concepts and Perspectives*; VCH: Weinheim, Germany, 1995. (b) Lehn, J.-M. *Angew. Chem., Int. Ed. Engl.* **1990**, *29*, 1304.

(4) Constable, E. C. In *Comprehensive Supramolecular Chemistry*; Atwood, J. L., Davies, J. E. D., Lehn, J.-M., MacNicol, D. D., Vögtle, F., Eds.; Pergamon Press: Oxford, U.K., 1996; Vol. *9*, p 213.

(5) (a) Constable, E. C. *Prog. Inorg. Chem.* **1994**, *42*, 67. (b) Baxter, P. N. W.; Lehn, J.-M.; Kneisel, B. O.; Fenske, D. *Chem. Commun.* **1997**, 2231. (c) Baxter, P. N. W.; Lehn, J.-M.; Decian, A.; Fischer, J. *Angew. Chem., Int. Ed. Engl.* **1993**, *32*, 1304.

(6) (a) Zhang, Z.; Dolphin, D. *Chem. Commun.* **2009**, 6931. (b) Albrecht, M.; Janser, I.; Houjou, H.; Fröhlich, R. *Chem.—Eur. J.* **2004**, *10*, 2839. (c) Albrecht, M.; Fröhlich, R. *J. Am. Chem. Soc.* **1997**, *119*, 1656. (d) Kersting, B.; Meyer, M.; Powers, R. E.; Raymond, K. N. *J. Am. Chem. Soc.* **1996**, *118*, 7221. (e) Piguet, C.; Bernardinelli, G.; Bocquet, B.; Quattropani, A.; Williams, A. F. *J. Am. Chem. Soc.* **1992**, *114*, 7440.

(7) Lehn, J.-M.; Rigualt, A.; Seigel, J.; Harrowfield, J.; Chevrier, B.; Moras, D. *Proc. Natl. Acad. Sci. U.S.A.* **1987**, *84*, 2565.

(8) (a) Glasson, C. R. K.; Lindoy, L. F.; Meehan, G. V. *Coord. Chem. Rev.* **2008**, *252*, 940. (b) Kaes, C.; Katz, A.; Hosseini, M. W. *Chem. Rev.* **2000**, *100*, 3553.

(9) (a) Riis-Johamnessen, T.; Harding, L. P.; Jeffery, J. C.; Moon, R.; Rice, C. R. *Dalton Trans.* **2007**, 1577. (b) Jeffery, J. C.; Riis-Johannessen, T.; Anderson, J. C.; Adams, C. J.; Robinson, A.; Argent, S. P.; Ward, M. D.; Rice, C. R. *Inorg. Chem.* **2007**, *46*, 2417. (c) Cantuel, M.; Gumy, F.; Bünjli, J.-C. G.; Piguet, C. *Dalton Trans.* **2006**, 2647. (d) Nitschke, J. R. *Acc. Chem. Res.* **2007**, *40*, 103.

(10) (a) Harding, L. P.; Jeffery, J. C.; Riis-Johannessen, T.; Rice, C. R.; Jeng, Z. T. *Chem. Commun.* **2004**, 654. (b) Harding, L. P.; Jeffery, J. C.; Riis-Johannessen, T.; Rice, C. R.; Jeng, Z. T. *Dalton Trans.* **2004**, 2396. (c) Campos-Fernandez, C. S.; Schottel, B. L.; Chifotides, H. T.; Bera, J. K.; Baska, J.; Coomen, J. M.; Russel, D. H.; Dunbar, K. R. *J. Am. Chem. Soc.* **2005**, *127*, 12909. (d) Argent, S. P.; Adams, H.; Riis-Johannessen, T.; Jeffery, J. C.; Harding, L. P.; Mamula, O.; Ward, M. D. *Inorg. Chem.* **2006**, *45*, 3905. (e) Habermehl, N. C.; Angus, P. M.; Kilah, N. L.; Norén, L.; Rae, A. D.; Willis, A. C.; Wild, S. B. *Inorg. Chem.* **2006**, *45*, 1445.

(11) (a) Lo, K. K.-W.; Hui, W.-K.; Chung, C.-K.; Tsang, K. H.-K.; Ng, D.-M.; Zhu, N.; Cheung, K.-K. *Coord. Chem. Rev.* **2005**, *249*, 1434. (b) Bignozzi, C. A.; Argazzi, R.; Kleverlaan, C. J. *Chem. Soc. Rev.* **2000**, *29*, 87. (c) Ford, P. C.; Cariati, E; Bourassa, J. *Chem. Rev.* **1999**, *99*, 3625.

(12) (a) Roundhill, D. M. *Photochemistry and Photophysics of Metal Complexes*; Plenum Press: New York, 1994. (b) Balzani, V.; Compagna, S.; Denti, G.; Juris, A.; Serroni, S.; Venturi, M. *Acc. Chem. Res.* **1998**, *31*, 26. (c) McMillin, D. R.; McNett, K. M. *Chem. Rev.* **1998**, *98*, 1201. (d) Ruthkosky, M.; Kelly, C. A.; Castellano, F. N.; Meyer, G. J. *Coord. Chem. Rev.* **1998**, *171*, 309.

(13) (a) Alstrum-Acevedo, J. H.; Brennaman, M. K.; Meyer, T. J. *Inorg. Chem.* **2005**, *44*, 6802. (b) Grätzel, M. *Inorg. Chem.* **2005**, *44*, 6841. (c) Meyer, G. J. *Inorg. Chem.* **2005**, *44*, 6852. (d) Evans, R. C.; Douglas, P.; Winscom, C. J. *Coord. Chem. Rev.* **2006**, *250*, 2093. (e) Benniston, A. C. *Chem. Soc. Rev.* **2004**, *33*, 573. (f) Coe, B. J.; Curati, N. R. M. *Comments Inorg. Chem.* **2004**, *25*, 147. (g) Demas, J. N.; DeGraff, B. A. *Coord. Chem. Rev.* **2001**, *211*, 317.

(14) (a) McGauhey, O.; Ros-Lis, J. V. *Anal. Chim. Acta* **2006**, *573*, 57. (b) Bossmann, S. H.; Turbo, C.; Schnabel, C.; Pokhrel, M. R.; Payawan, L. M.; Baumeister, B.; Worner, M. *J. Phys. Chem. B* **2001**, *105*, 5374. (c) Deronzier, A.; Moutet, J.-C. In *Comprehensive Coordination Chemistry*, 2nd ed.; Ward, M. D., Ed.; Elsevier: Oxford, U.K.; 2004; Vol. *9*, p 471. (d) Suzuki, M.; Waraska, C. C.; Mallouk, T. E.; Nakayama, H.; Hanabusa, K *J. Phys. Chem.* **2002**, *106B*, 4227.

(15) (a) Yu, G.; Yin, S.; Liu, Y.; Shuai, Z.; Zhu, D. *J. Am. Chem. Soc.* **2003**, *125*, 14816. (b) Pang, J.; Marcotte, E. J.-P.; Seward, C.; Brown, R. S.; Wang, S. *Angew. Chem., Int. Ed.* **2001**, *40*, 4042. (c) Seward, C.; Pang, J.; Wang, S. *Eur. J. Inorg. Chem.* **2002**, *6*, 1390. (d) Ma, Y.; Chao, H.-Y.; Wu, Y.; Lee, S. T.; Yu, W.-Y.; Che, C.-M. *Chem. Commun.* **1998**, 2491.

(16) Son, H.-J.; Han, W.-S.; Chun, J.-Y.; Kong, B.-K.; Know, S.-N.; Ko, J.; Han, S. J.; Lee, C.; Kim, S. J.; Kang, S. O. *Inorg. Chem.* **2008**, *47*, 5666.

(17) (a) Kunkely, H.; Vogler, A. *J. Chem. Soc., Chem. Commun.* **1990**, 1204. (b) Vogler, A.; Ford, P. C. *Acc. Chem. Res.* **1993**, *26*, 220. (c) Che, C.-M.; Kwong, H.-L.; Yam, V. W.-W.; Cho, C.-K. *J. Chem. Soc., Chem. Commun.* **1989**, 855. (d) Xino, H.; Cheung, K.-K.; Guo, C.-X.; Che, C.-M. *J. Chem. Soc., Dalton. Trans.* **1994**, 1867. (e) Tzeng, B.-C.; Che, C.-M.; Peng, S.-M. *Chem. Commun.* **1997**, 1771. (f) Yang, W.; Schmider, H.; Wu, Q.; Zang, Y.-S.; Wang, S. *Inorg. Chem.* **2000**, *39*, 2397.

(18) (a) Schottel, B. L.; Chifotides, H. T.; Dunbar, K. R. *Chem. Soc. Rev.* **2008**, *37*, 68. (b) Mascal, M.; Yakovlev, I.; Nikitin, E. B.; Fettinger, J. C. *Angew. Chem., Int. Ed.* **2007**, *46*, 8782. (c) Schottel, B. L.; Chifotides, H. T.; Shatruk, M.; Chauai, A.; Perez, L. M.; Bacsa, J.; Dunbar, K. R. *J. Am. Chem. Soc.* **2006**, *128*, 5895. (d) Maheswari, P. U.; Modec, B.; Pevec, A.; Kozlevcar, B.; Massera, C.; Gamez, P.; Reedijk, J. *Inorg. Chem.* **2006**, *45*, 6637. (e) Barrios, L. A.; Aromi, G.; Frontera, A.; Quiñonero, D.; Deyá, P. M.; Gamez, P.; Roubeak, O.; Shatton, E. J.; Teat, S. J. *Inorg. Chem.* **2008**, *47*, 5873. (f) Capó, M.; Benet-Buchholz, J.; Ballester, P. *Inorg. Chem.* **2008**, *47*, 10190. (g) Gamez, P.; Mooibroek, T. J.; Teat, S. J.; Reedijk, J. *Acc. Chem. Res.* **2007**, *40*, 435. (h) Domasevitch, K. V.; Solntsev, P. V.; Gural'skiy, I. A.; Krautscheid, H.; Rusanov, E. B.; Cheranega, A. N.; Howard, J. A. K. *Dalton Trans.* **2007**, 3893. (i) Manzano, B. R.; Jalon, F. A.; Ortiz, I. M.; Sariano, K. L.; dela Torre, F. G.; Elguero, J.; Maestro, M. A.; Mereiter, K.; Claridge, T. D. W. *Inorg. Chem.* **2008**, *47*, 413. (j) Gural'skiy, I. A.; Solntsev, P. V.; Krautscheid, H.; Domasevitch, K. V. *Chem. Commun.* **2006**, 4808. (k) de Hoog, P.; Gamez, P.; Mutikainen, I.; Turpeinen, U.; Reedijk, J. *Angew. Chem., Int. Ed.* **2004**, *43*, 5815. (l) Demeshko, S.; Dechart, S.; Meyer, F. *J. Am. Chem. Soc.* **2004**, *126*, 4508. (m) Berryman, O. B.; Hof, F.; Hynes, M. J.; Johnson, D. W. *Chem. Commun.* **2006**, 506. (n) Mooibroek, T. J.; Black, C. A.; Gamez, P.; Reedijk, J. *Cryst. Growth Des.* **2008**, *8*, 1082.

(19) Gamez, P.; Reedijk, J. *Eur. J. Inorg. Chem.* **2006**, 29.

(20) (a) Mooibroek, T. J.; Teat, S. J.; Massera, C.; Gamez, P.; Redijk., J. *Cryst. Growth Des.* **2006**, *6*, 1569. (b) Sarkhel, S.; Rich, A.; Egli, M. *J. Am. Chem. Soc.* **2003**, *125*, 8998. (c) Berger, I.; Egli, M. *Chem.—Eur. J.* **1997**, *3*, 1400. (d) Gung, B. W.; Xue, X. W.; Reich, H. *J. Org. Chem.* **2005**, *70*, 7232.

(21) Meyer, E. A.; Castellano, R. K.; Diederich, F. *Angew. Chem., Int. Ed.* **2003**, *42*, 1210.

(22) Kundu, N. Ph.D. Thesis, Jadavpur University, Kolkata, India, 2009.

(23) Knueppel, D.; Martin, S. F. *Angew. Chem., Int. Ed.* **2009**, *48*, 2569.

(24) Kundu, N.; Maity, M.; Chatterjee, P. B.; Teat, S. J.; Endo, A.; Chaudhury, M. *J. Am. Chem. Soc.* **2011**, *133*, 20104.

(25) Perrin, D. D.; Armarego, W. L. F.; Perrin, D. R. *Purification of Laboratory Chemicals*, 2nd ed.; Pergamon: Oxford, U.K., 1980.

(26) Robinson, W. R. *J. Chem. Educ.* **1985**, *62*, 1001.

(27) Audhya, A.; Maity, M.; Bhattacharya, K.; Clérac, R.; Chaudhury, M. *Inorg. Chem.* **2010**, *49*, 9026.

(28) Gagné, R. R.; Kovel, C. A.; Lisensky, G. C. *Inorg. Chem.* **1980**, *19*, 3854.

(29) Sheldrick, G. M. *SADABS, Program for Empirical Absorption Correction of Area Detector Data*; University of Göttingen: Göttingen, Germany, 1996.

(30) Sheldrick, G. M. *Acta Crystallogr.* **1990**, *46A*, 467.

(31) Sheldrick, G. M. *SHELXL-97, Program for Crystal Structure Refinements*; University of Göttingen: Göttingen, Germany, 1997.

(32) *SAINT*, version 6.02; Bruker AXS Inc.: Madison, WI, 2002.

(33) *DIAMOND, Visual Crystal Structure Information System*, version 3.1; Crystal Impact: Bonn, Germany, 2004.

(34) (a) Constable, E. C.; Elder, S. M.; Healy, J.; Tocher, D. A. *J. Chem. Soc., Dalton. Trans.* **1990**, 1669. (b) Constable, E. C.; Lewis, J.; Liptrot, M. C.; Raithby., P. R. *Inorg. Chim. Acta* **1990**, *178*, 47. (c) Merritt, L. L.; Schroeder, E. D. *Acta Crystallogr.* **1956**, *9*, 801. (d) Nakatsu, K.; Yoshioka, H.; Matsui, M.; Koda, S.; Ooi, S. *Acta. Crystallogr., Sect. A* **1972**, *28*, S24.

(35) Nakamoto, K. *Infrared and Raman Spectra of Inorganic and Coordination Compounds*, 5th ed.; VCH-Wiley: New York, 1997.

(36) Yang, W.; Schmider, H.; Wu, Q.; Zhang, Y.-S.; Wang, S. *Inorg. Chem.* **2000**, *39*, 2397.

(37) (a) Jeffrey, G. A. *An Introduction to Hydrogen Bonding*; Oxford University Press: New York, 1997; p 12. (b) Steed, J. W.; Atwood, J. L. *Supramolecular Chemistry*; John Wiley and Sons, Ltd.; Chichester, U.K., 2000. (c) Desiraju, G. R. *Chem. Commun.* **2005**, 2995.

(38) Fan, R.-Q.; Zhu, D.-S.; Mu, Y.; Li, G.-H.; Yang, Y.-L.; Su, Q.; Feng, S.-H. *Eur. J. Inorg. Chem.* **2004**, 4831.
(39) Fu, Z.; Gao, S.; Liu, S. *Acta Crystallogr.* **2007**, *C 63*, m 459.
(40) (a) Lavallee, D. K.; Baughman, M. D.; Phillips, M. P. *J. Am. Chem. Soc.* **1997**, *99*, 718. (b) Piguet, C.; Bernardinelli, G.; Williams, A. F. *Inorg. Chem.* **1989**, *28*, 2920. (c) Rüttimann, S.; Piguet, C.; Bernardinelli, G.; Bocquet, B.; Williams, A. F. *J. Am. Chem. Soc.* **1992**, *114*, 4230.
(41) Brown, E. R.; Large, R. F. Electrochemical Methods. In *Physical Methods in Chemistry*; Weissberger, A., Rossiter, B., Eds.; Wiley-Interscience: New York, 1971; Part IIA, Chapter VI.

dx.doi.org/10.1021/ic202595p | *Inorg. Chem.* 2012, 51, 2652−2661